Botanical Studies (2008) 49: 199-213.

Isolation, characterization and phosphate-starvation inducible expression of potential *Brassica napus PURPLE ACID PHOSPHATASE 17* (*BnPAP17*) gene family

Kun LU[1,3], Jia-Na LI [1,3], Wei-Ran ZHONG[1], Kai ZHANG[1], Fu-You FU[2], and You-Rong CHAI[1,3,*]

[1]*Chongqing Rapeseed Technology Research Center; Chongqing Key Laboratory of Crop Quality Improvement; Key Lab of Biotechnology & Crop Quality Improvement of Ministry of Agriculture; College of Agronomy and Biotechnology, Southwest University, Tiansheng Road 216#, Beibei, Chongqing, 400716, P. R. China*

[2]*State Key Laboratory of Plant Genomics, Institute of Genetics and Developmental Biology, Chinese Academy of Sciences, Beijing 100101, P. R. China*

(Received September 20, 2007; Accepted February 26, 2008)

ABSTRACT. Three members of a *Brassica napus PURPLE ACID PHOSPHATASE 17* (*BnPAP17*) gene family were isolated. The full-length cDNAs of *BnPAP17-1*, *BnPAP17-2* and *BnPAP17-3* are 1277, 1356 and 1349 bp, with corresponding genomic sequences of 1466, 1594 and 1598 bp, respectively. The deduced 337-aa BnPAP17-1, 333-aa BnPAP17-2 and 333-aa BnPAP17-3 proteins are all secretary low molecular weight (LMW) PAPs, containing a metallophos domain, 5-block conserved motifs and 7 metal-ligating residues. *BnPAP17-2* and *BnPAP17-3* are highly similar to each other, but distinct from *BnPAP17-1*. Southern analysis suggests that these three genes comprise the entire *BnPAP17* gene family. They are all mainly transcribed in reproductive organs especially in bud. In vegetative organs, *BnPAP17-2* and *BnPAP17-3* are expressed in root, hypocotyl and stem, while *BnPAP17-1* expression is limited to root. In seedlings, these genes are all strongly induced by phosphate-starvation, and return to basal levels after phosphate resupply. Thus they are suggested to play important roles in reproductive development and adaptation to phosphorus deficiency.

Keywords: *Brassica napus*; Gene family; Purple acid phosphatase; Phosphate starvation.

Abbreviations: aa, amino acid; **bp,** base pair; **DOI,** days of induction; **DOR,** days of Pi resupply; **HOI,** hours of induction; **ORF,** open reading frame; **P,** phosphorus; **PAP,** purple acid phosphatase; **Pi,** phosphate; **RACE,** rapid amplification of cDNA ends.

Database Accession Nos: **EU107164** (BnPAP17-1 gene), **EU107165** (BnPAP17-1 mRNA), **EU107166** (BnPAP17-1 premature mRNA), **EU107167** (BnPAP17-2 gene), **EU107168** (BnPAP17-2 mRNA), **EU107169** (BnPAP17-3 gene), and **EU107170** (BnPAP17-3 mRNA).

INTRODUCTION

Purple acid phosphatases (PAPs; E.C. 3.1.3.2) are a class of tartrate-resistant enzymes that contain a metal-binding dinuclear center in their active sites and catalyze the hydrolysis of activated phosphoric acid esters and anhydrides at a pH range from 4 to 7 (Klabunde et al., 1995). These enzymes are readily distinguished from other acid phosphatases (APases) by their characteristic purple color, which is attributed to a charge transfer from tyrosine to Fe(III) at ~560 nm (Vincent et al., 1992). The *Arabidopsis thaliana* genome is annotated with 29 PAPs, while only 1 histidine APase, 4 vegetative storage protein type of APases, and 10 phosphatidic APases, suggesting that *PAP* genes may play crucial roles in plant P metabolism (Li et al., 2002).

PAPs from animals, plants and microbes have been isolated and characterized (Schenk et al., 2000b). The mammalian PAPs are monomeric proteins of approximately 35 kDa and exist in 2 forms: an oxidized, purple form containing an Fe(III)-Fe(III) center, which exhibits little if any catalytic activity; and a pink, reduced form containing a mixed-valent Fe(III)-Fe(II) center, which is the enzymatically active species (Vincent et al., 1992). They mainly distribute in porcine uterine fluid (uteroferrin, Uf), bovine spleen, human bones and macrophages, and function in *in vivo* iron transport, bone resorption, antigen presentation and some redox reactions (Olczak et al., 2003).

[3]These authors have equal contribution to the study.

*Corresponding author: E-mail: chaiyourong1@163.com; ljn1950@swu.edu.cn; Tel: +86-23-68250744, Fax: +86-23-68251950.

In plants, PAPs have been divided into 2 groups: high molecular weight (HMW) and low molecular weight (LMW) PAPs. Plant HMW PAPs are homodimeric proteins with ~55-kDa subunits. The precise crystal structures, biochemical and biophysical properties of plant HMW PAPs have been studied in a few instances, such as the KbPAP (**P80366**) from red kidney bean and IbPAP1 (**AAF19821**) from sweet potato (Strater et al., 1995; Schenk et al., 2005). Though many plant HMW *PAP* genes have been obtained, their biological functions remain poorly known. The *LaSAP1* mRNA (**AB023385**) from white lupin accumulated in both roots and shoots under Pi deficient conditions, while *LaSAP2* (**AB037887**) was only induced in roots. Mature LaSAP1 and LaSAP2 were suggested to be located to plasma membrane and extracellular respectively (Wasaki et al., 1999; Wasaki et al., 2000). Potato *StPAP1* (**AY598343**) encodes a LMW PAP similar to mammalian PAPs, and is highly expressed in stem and root and insensitive to Pi-starvation, while *StPAP2* (**AY598341**) and *StPAP3* (**AY598342**) encode 2 typical plant HMW PAPs, and are induced by Pi deprivation in roots or both stem and roots respectively (Zimmermann et al., 2004). Under low-Pi conditions, the transcript level of alfalfa *MtPAP1* (**AY804257**) was reduced in leaves and increased in roots, with the strongest signal detected in roots. *MtPAP1* may function to improve P acquisition in plants under Pi stress (Xiao et al., 2006). In *Arabidopsis*, *AtPAP11* (**NM_127370**) and *AtPAP12* (**NM_128277**) were up-regulated by Pi deficiency (Li et al., 2002). Further study on *AtPAP12* promoter showed that it was specifically activated by Pi-starvation, while salicylic or jasmonic acids and other inducers of gene expression could not activate it (Haran et al., 2000). NaCl stress and oxidative stress but not Pi-starvation induced the expression of soybean *GmPAP3* (**AY151271**) which exhibited phytase activity in germination (Liao et al., 2003). Moreover, two isoforms of tobacoo PAPs, NtPAP12 (**BAC55155**) and NtPAP21 (**BAC55157**), were associated with cell wall generation (Kaida et al., 2003). These studies indicate that plant HMW PAPs are multi-functional proteins, which are necessary for plant P metabolism and adaptation to low P conditions.

Plant LMW PAPs are much less well characterized than plant HMW PAPs. Except for AtPAP17 (AtACP5, **NP_566587**), most LMW PAPs are deduced from corresponding cDNAs, e.g. AtPAP3 (**NP_172923**), AtPAP4 (**NP_173894**), AtPAP7 (**NP_178297**), AtPAP8 (**NP_973397**) from *A. thanalia*, GmPAP (**AAF60316**) from soybean, IbPAP (**AAF60315**) from sweet potato, PvPAP (**AAF60317**) from common bean, and StPAP1 (**AAT37529**) from potato (Del Pozo et al., 1999; Oddie et al., 2000; Li et al., 2002; Zimmermann et al., 2004). AtPAP17 was purified as a 34-kDa monomer, containing 5-block conserved motifs and 7 metal-binding sites, and its C-terminal sequence showed significant similarity with mammalian PAPs. *AtPAP17* transcript accumulation is strongly induced by Pi starvation and is also responsive to salt stress, abscisic acid, peroxide and senescence (Del Pozo et al., 1999). Consequently, *AtPAP17* has been regarded as an important control index in several Pi metabolism researches (Muller et al., 2004; Todd et al., 2004).

Rapeseed (*Brassica napus*) is the second largest oil bearing crop in the world, and is the most widely grown oil crop in China (Yang et al., 2007). However, it is sensitive to Pi limitation, which has become a crucial yield-limiting factor for this crop, especially in the Yangtze River rapeseed belt, despite the increased use of Pi fertilizers (Guo et al., 2002). Owing to strong interactions of Pi with other metal ions in soils, the majority of soil Pi is locked in organic and immobile inorganic complexes. Less than 20% of applied fertilizer Pi could be assimilated by crops during the first growth season, leading to an excess amount of soil Pi that contributes to environmental problems such as Pi-enrichment of water ecosystems. Screening of P-efficient *B. napus* genotypes and study of their adaptation mechanism to Pi-starvation are basic strategies to improve Pi utilization efficiency as well as reduce Pi-related water contamination with limited application of non-renewable Pi-fertilizers. Here we report the isolation, molecular characterization, and Pi-starvation induced expression of the 3-member *B. napus PAP17* (*BnPAP17*) gene family that is othologous to *AtPAP17*, which adds clues for functional and evolutionary characterization of plant *PAP17* genes and molecular biological elucidation of Pi-deficiency responses in rapeseed.

MATERIALS AND METHODS

Plant materials

Seed of inbred line W17 of typical *B. napus* genetic type (AACC, 2n=4x=38) were kept by Chongqing Rapeseed Technology Research Center and grown under normal field conditions. Root (Ro), hypocotyl (Hy), cotyledon (Co), stem (St), leaf (Le), bud (Bu), flower (Fl), silique pericarp (SP), and seed of 10 (10D), 20 (20D) and 30 d (30D) after flowering were sampled. For Pi-starvation treatment, W17 seedlings were cultured in full-strength Hoagland's solution with a cycle of 16 h of artificial light at 25°C and 8 h dark at 18°C (Hoagland and Arnon, 1950). Four-week old seedlings were subjected to Pi-starvation treatment (0.5 μM KH_2PO_4), and seedling leaves (SL) and seedling roots (SR) were harvested after 0 h, 12 h, 24 h, 2 d, 4 d and 8 d of treatments respectively, and sampled again after 4 d of Pi resupply. All samples were immediately frozen in liquid nitrogen, and stored at -80°C.

Isolation of total RNA and DNA

Total genomic DNA was isolated from mixed young leaves of 3 representative plants using a CTAB-based method (Saghai-Maroof et al., 1984), while total RNA from various organs was isolated using a slightly modified CTAB method (Jaakola et al., 2001). Total RNA from SR and SL was extracted using the Plant RNA Mini Kit (Watson Biotechnologies, Inc., China). Each RNA sample

was treated with RNase-free DNase I (TaKaRa) to remove contaminating DNA. Quality and concentration of total RNA and genomic DNA samples were assessed by agarose gel electrophoresis and spectrophotometry, and stored at -80°C.

Amplification of the 3′ and 5′ cDNA ends of *BnPAP17* genes

RACE-ready total first-strand cDNA was synthesized from 5 μg of equally proportioned (w/w) mixture of total RNA from SR and SL induced by varied degrees of Pi-starvation using the GeneRacer kit (Invitrogen, USA). According to multi-alignment of 29 *A. thaliana PAP* genes, the sites conserved in *AtPAP* genes and specific for *AtPAP17* were chosen to design conserved-site primers for amplification of 3′ and 5′ cDNA ends of *BnPAP17* genes.

For 3′-RACE, conserved-site sense primers FPAP17-31 (5′-AGCAAGATGGAAGATTGTTGTTGG-3′) and FPAP17-32 (5′-GAACGGTGTTGATCTCTACATGA AT-3′) were designed. Using primers FPAP17-31 and GeneRacer™ 3′ Primer (5′-GCTGTCAACGATACG CTACGTAACG-3′), the 50-μl primary polymerase chain reaction (PCR) was conducted using 2 μl of total first-strand cDNA as template on a MyCycler gradient thermocycler (Bio-Rad, USA): predenaturation at 94°C for 2 min, followed by 30 cycles of amplification (94°C for 1 min, 52°C for 1 min, and 72°C for 1 min), and by 72 °C for 10 min. Then 0.2 μl of primary PCR product was used as template for nested PCR using primers FPAP17-32 and GeneRacer™ 3′ Nested Primer (5′-CGCTACGTAA CGGCATGACAGTG-3′) with other conditions similar to the primary PCR. In 5′-RACE, kit primers GeneRacer™ 5′ Primer (5′-CGACTGGAGCACGAGGACACTGA-3′) and GeneRacer™ 5′ Nested Primer (5′-GGACACTGACA TGGACTGAAGGAGTA-3′) were paired with conserved-site antisense primers RPAP17-51 (5′-GAGTCGTGTCA ACAAAGAACATCTC-3′) and RPAP17-52 (5′-GAAG ACTTGGAGCAGTGTAGATGTTA-3′) for primary and nested PCRs respectively, with other conditions identical to those for 3′ primary PCR. PCR products were gel purified then subcloned into pMD18-T vector (TaKaRa), and transformed into *E. coli* DH5α. Positive colonies were sequenced using primers M13F and M13R at Invitrogen Corporation, Shanghai, China.

Amplification of full-length cDNAs and genomic sequences of *BnPAP17* genes

Sense primers FPAP17-7 (5′-ATTTCCTTCTCCCT CCCTCCC-3′) and FPAP17-12 (5′-ATCATCATCCTTC GCACCTTAACC-3′), and antisense primers RPAP17-9 (5′- AATGCATTTGACTATAACATTAAGAAGATAAT C-3′) and RPAP17-19 (5′-GATAGGGATGCTAAACTT ATCTTAAATATATG-3′), were designed corresponding to the utmost ends of the sequenced 5′- and 3′-RACE products respectively. Primers were combined into 4 pairs, FPAP17-7/RPAP17-9, FPAP17-12/RPAP17-9, FPAP17-7/ RPAP17-19 and FPAP17-12/RPAP17-19, for amplification of full-length cDNAs of *BnPAP17* members. In each 50-μl PCR, 0.5 μl of first-strand total cDNA was used as template. After 2 min at 94°C, 35 cycles of amplification were performed (94°C for 1 min, 52°C for 1 min, 72°C for 2 min), followed by 72°C for 10 min. Primer combinations successful in full-length cDNA amplifications were used to amplify the corresponding genomic sequences by replacing the template with 0.5 μg of total genomic DNA of line W17 under the same conditions. PCR products were purified and subcloned, followed by sequencing.

Bioinformatic analysis

Sequence alignment, ORF translation, and calculation of obtained sequences were conducted using Vector NTI Advance program v. 10.3.0 (Invitrogen, USA). BLAST and Conserved Domain search were carried out on the NCBI website (http://www.ncbi.nlm.nih.gov). Protein structures were predicted using online bioinformatic tools linked by Expasy (http://www.expasy.org) and SoftBerry (http://www.softberry.com) websites. BnPAP17 proteins and other PAPs retrieved from GenBank were aligned with ClustalX program v. 1.83. Subsequently, a phylogenetic tree was constructed using Neighbor-Joining method with MEGA program v. 3.1 (Thompson et al., 1997; Kumar et al., 2004). The reliability of the tree was measured by bootstrap testing with 1000 replicates.

Southern hybridization detection

Sixty-μg aliquots of genomic DNA of line W17 were digested overnight at 37°C with either *Dra*I, *Eco*RI, *Eco*RV, *Sac*I or *Xba*I (New England BioLabs, USA) respectively. None of these enzymes cut within the hybridization region of cloned *BnPAP17* members. Digested DNA samples were fractionated by electrophoresis on 0.8% agarose gel, transferred to a positively charged nylon membrane (Roche, Germany) through standard capillarity method. Using primers FPAP17S (5′-CGTTAAAGAATA CTACACAGAAGAAG-3′) and RPAP17S (5′-GTGGCCTTGGATCTTTTTAAGG-3′), a 126-bp highly conserved fragment was amplified using *BnPAP17-1* full-length cDNA as template at an annealing temperature of 58°C and labeled with Digoxigenin-11-dUTP using PCR DIG Probe Synthesis Kit (Roche, Germany). Hybridization was performed at 40.5°C for 16 h (DIG Easy Hyb, Roche, Germany). Membrane washing and immunological detection (DIG Wash and Block Buffer Set and DIG Nucleic Acid Detection Kit, Roche, Germany) were carried out according to the manufacturer's protocols.

RT-PCR detection of tissue specificities and Pi-starvation induced expression patterns of *BnPAP17* genes

Semi-quantitative reverse transcription-PCR (RT-PCR) was adopted to detect the expression profiles of the 3 *BnPAP17* members in 11 organs. One-μg aliquots of total RNA extracted from each sample

were used as templates in reverse transcription with the Oligo dT-Adaptor Primer using RNA PCR Kit (AMV) Ver. 3.0 (TaKaRa). The RT-PCR reaction for a house-keeping gene using specific primers F26S (5′-CACAATGATAGGAAGAGCCGAC-3′) and R26S (5′-CAAGGGAACGGGCTTGGCAGAATC-3′) designed according to a 534-bp conserved region of *A. thaliana 26S rRNA* gene was performed to monitor sample uniformity of initial RNA input and RT efficiency (Singh et al., 2004). RT-PCRs were carried out in a 25-µl volume. *26S rRNA* gene amplification was performed under the following condition: 94°C for 2 min, followed by 21 cycles of amplification (94°C for 1 min, 60°C for 1 min and 72°C for 1 min), then 72°C for 10 min. Primer pairs FPAP17-1S (5′-TCCCTTCTCTTCTTTGCTTCGCAT-3′) / RPAP17-52, FPAP17-23S (5′-ACAATCAGTCTGTTG TGGCCTAC-3′) / RPAP17-2S (5′-AGTGGTCGTGTCC ATTCATATAG-3′), and FPAP17-23S / RPAP17-3S (5′-CAGTGGTCATGTCCATTCATGTAA-3′) were used for member-specific detection of *BnPAP17-1*, *BnPAP17-2* and *BnPAP17-3* respectively. Based on gradient PCR results using W17 genomic DNA as template, the highest annealing temperatures for efficient exponential amplification of the 3 primer pairs were determined as 60 °C, 61°C and 61°C respectively, and the specificity was proved by no cross amplification among the 3 members using colony plasmids as templates. For investigation of expression patterns of *BnPAP17* members under Pi-starvation stress conditions, RNA samples from SR and SL of different treatments were reverse-transcribed and genes were amplified for 31 cycles respectively using above conditions. PCR products were detected with agarose gel electrophoresis and analyzed with UTHSCSA ImageTool for Windows v. 3.00. In order to control experimental error, all RT-PCRs were done with 3 replicates.

RESULTS

Isolation of full-length cDNAs and genomic sequences of 3 *BnPAP17* genes

5′-RACE yielded 6 products that appear to represent 2 different genes. One gene was represented by products of 496, 498, 499 and 529 bp, which were identical to each other except for alternative initiation sites, and another 605-bp product that shared sequence identity but possessed a 109-bp unspliced intron corresponding to the 1st intron of *AtPAP17*. The second gene was represented by a related but unique 488-bp product. NCBI BLASTn indicated that all of the 5′ cDNA products showed highest identities to *AtPAP17* mRNA (**NM_112660**).

3′-RACE also yielded 6 products, all of which share identity with *AtPAP17*. These products also appear to represent 2 different genes, one corresponding to 4 fragments (363, 360, 359 and 354 bp, poly A tail not included) and another corresponding to 2 fragments (483 and 462 bp), with alternative polyadenylation sites in each gene.

Four pairs of primers designed based on 5′- and 3′-RACE results were used to amplify full-length cDNAs. Only primer pairs FPAP17-7 / RPAP17-19 and FPAP17-12 / RPAP17-9 yielded specific products. Amplification with primer pair FPAP17-7 / RPAP17-19 resulted in a 1277-bp unique full-length cDNA named *BnPAP17-1*, while amplification with primer pair FPAP17-12 / RPAP17-9 yielded 2 homologous but obviously distinct full-length cDNAs named *BnPAP17-2* (1356 bp) and *BnPAP17-3* (1349 bp). No full-length cDNA clone was identified that retained intron I, suggesting that the non-excision event detected with 5′-RACE is rare. It is unknown if this event is biologically relevant. These same primer pairs were used to amplify genomic sequences corresponding to the above 3 full-length cDNAs by substituting the template with total genomic DNA of line W17. Gel detection indicated that primer pair FPAP17-7 / RPAP17-19 yielded a bright band of about 1450 bp, whereas a 1600-bp band for primer pair FPAP17-12 / RPAP17-9. Sequenced genomic sequences of *BnPAP17-1*, *BnPAP17-2* and *BnPAP17-3* were 1466 bp, 1594 bp and 1598 bp, respectively. The genomic sequences were identical to respective full-length cDNAs in exon regions.

Molecular characterization of nucleotide sequences of the 3 *BnPAP17* genes

Genomic sequences of all members of *BnPAP17* gene family contain 2 introns with standard GT…AG splicing boundaries at the positions of those of *AtPAP17*: 391-499 bp and 657-736 bp in *BnPAP17-1*, 350-510 bp and 668-744 bp in *BnPAP17-2*, and 350-509 bp and 667-755 bp in *BnPAP17-3* (Figure 1). The cDNA of *BnPAP17-1* possesses a 1014-bp ORF (with stop codon) flanked by a 189-bp 5′ UTR and a 74-bp 3′ UTR. The cDNAs of *BnPAP17-2* and *BnPAP17-3* both have a 160-bp 5′ UTR and a 1002-bp ORF, but differed in 3′ UTR length (187 bp for *BnPAP17-2* and 194 bp for *BnPAP17-3*). *BnPAP17-1* has 4 alternative transcriptional start sites at A_1, A_{31}, T_{32} and A_{34}, 4 alternative polyadenylation sites right after C_{1457}, C_{1462}, T_{1463} and C_{1466}, respectively, and a polyadenylation signal $A_{1404}TAAA_{1409}$. *BnPAP17-2* and *BnPAP17-3* both have 2 sites of polyadenylation signal AATAAA in their 3′ UTRs, and *BnPAP17-2* also possesses 2 alternative polyadenylation sites at T_{1579} and T_{1600}. Containing the 109-bp non-excised intron I, *BnPAP17-1PM* is 1386 bp and its ORF is pre-terminated by intron-derived stop codon TGA at 418-420 bp (Figure 1).

BnPAP17-2 and *BnPAP17-3* share as high as 95.8% genomic and 97.5% mRNA identities to each other, but they are quite divergent from *BnPAP17-1*. *AtPAP17*, *BnPAP17-1* and *BnPAP17-2*/*BnPAP17-3* form a nearly triangle relationship (Table 1).

Furthermore, PlantCARE (http://bioinformatics.psb.ugent.be/webtools/plantcare/html/) predicted that several types of *cis*-acting regulatory elements, such as light responsive elements Sp1, GT1-motif, I-box and TCCC-motif, core promoter element TATA-box and elements for

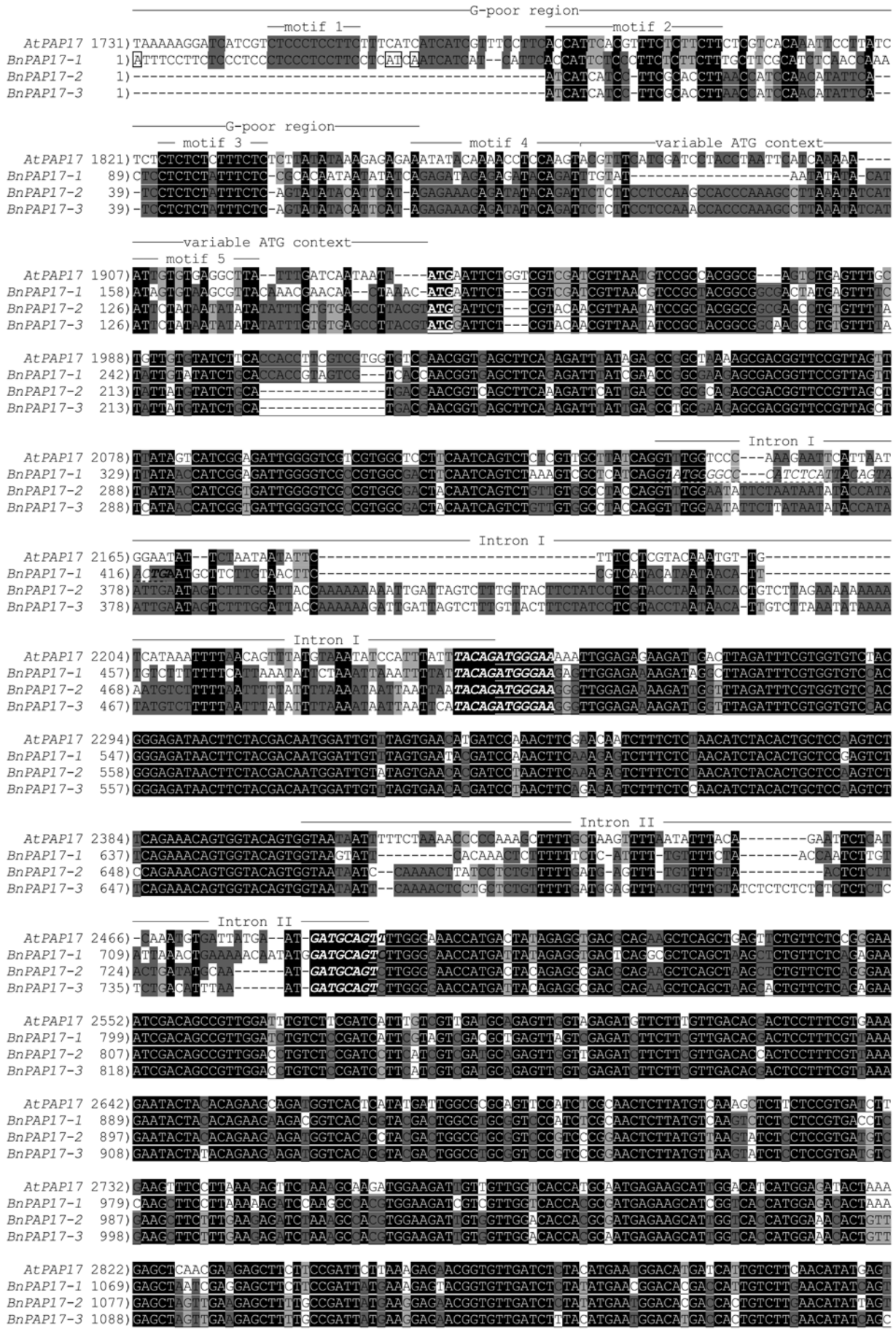
G-poor region
motif 1
motif 2
G-poor region
motif 3
motif 4
variable ATG context
variable ATG context
motif 5
Intron I
Intron I
Intron I
Intron II
Intron II
AtPAP17
BnPAP17-1
BnPAP17-2
BnPAP17-3

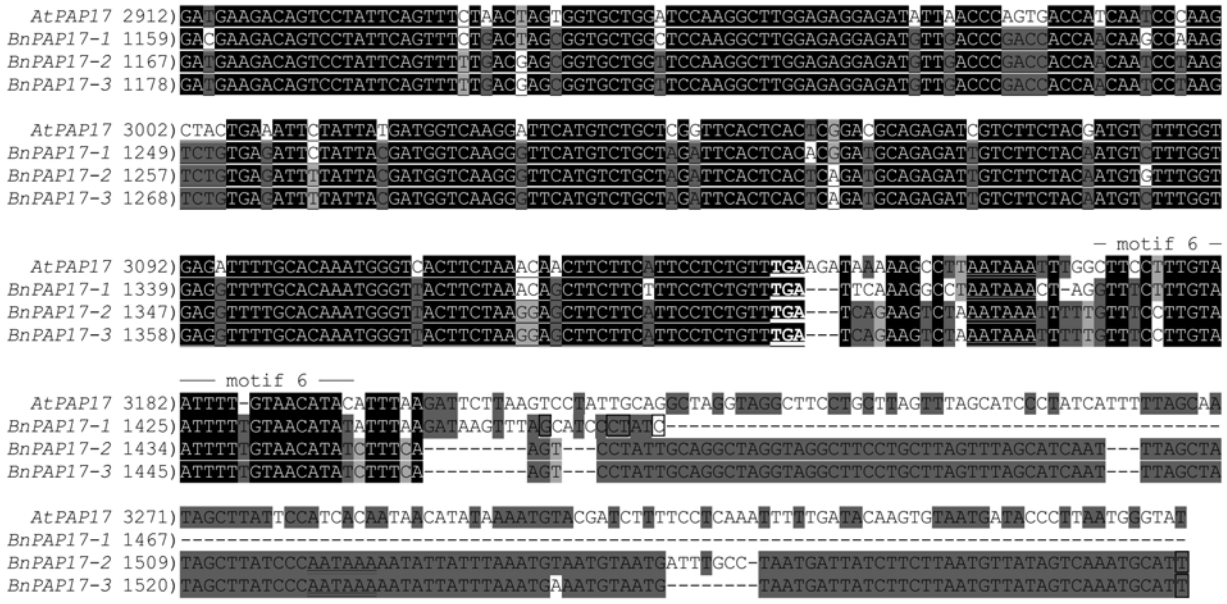

Figure 1. Nucleotide alignment of *AtPAP17* and the 3 *BnPAP17* genes. The coding regions are underlined, with the start codon ATG and the stop codon TGA in bold face and solid-underlined. The (alternative) initiation sites and (alternative) polyadenylation sites are boxed, and the putative polyadenylation signals are double-underlined. Two conserved 3′-intron|5′-exon boundary sequences are in bold italics. In 5′ and 3′ UTRs, conserved motifs (motifs 1-6), G-poor region and variable ATG context are marked. In *BnPAP17-1*, the bases in the first intron participating in coding and premature termination in *BnPAP17-1PM* mRNA are dash-underlined.

Table 1. Sequence homology of *BnPAP17* genes.

Identities (%) on genomic/mRNA level				Protein identities/similarities (%)			
	BnPAP17-1	*BnPAP17-2*	*BnPAP17-3*		BnPAP17-1	BnPAP17-2	BnPAP17-3
AtPAP17	77.2/80.5	73.5/77.1	73.4/77.0	AtPAP17	85.2/90.2	82.8/88.2	83.4/88.8
BnPAP17-1		77.0/81.9	77.2/82.1	BnPAP17-1		89.3/93.5	89.6/94.1
BnPAP17-2			95.8/97.5	BnPAP17-2			98.5/99.4

the anaerobic induction ARE and in endosperm expression GCN4_motif were identified in the leader sequences of the 3 *BnPAP17* genes, implying their possible regulation by a wide range of environmental signals.

Southern hybridization detection for possible members of *BnPAP17* gene family

Southern analysis was used to investigate the number of *BnPAP17* gene family members. Three distinct bands were detected for *Eco*RI, *Sac*I and *Xba*I digests, while 2 bands were detected for *Dra*I and *Eco*RV digests (Figure 6). Because these enzymes do not cut within the probed region of the 3 cloned *BnPAP17* genes, it is likely that the *BnPAP17* gene family consists of only the 3 members that were isolated in this study. It is possible that other gene members exist but these would have to share identical digestion patterns for all the 5 enzymes.

Conservation and features of the 3 deduced BnPAP17 proteins

The deduced BnPAP17-1, BnPAP17-2 and BnPAP17-3 proteins are 337, 333 and 333 aa respectively (Figure 2). BnPAP17-1 possesses a calculated MW of 38.24 kDa and a predicted isoelectric point (pI) value of 5.86, while BnPAP17-2 and BnPAP17-3 are 37.80 kDa and 37.82 kDa with pI values of 5.27 and 5.28 respectively. BnPAP17-1, BnPAP17-2 and BnPAP17-3 are rich in S (10.09%, 9.61% and 9.31% respectively). The ORF of *BnPAP17-1PM* encodes a polypeptide of only 76 residues with a Mw of 8.40 kDa and a pI of 9.11. Its first 67 residues are identical to those of BnPAP17-1, while the C-terminal 9 residues have no homology to known proteins since they are translated from the unspliced intron I.

BnPAP17 proteins show high similarities to one another and other plant PAPs. Homology analysis on protein sequences showed the same trend among BnPAP17-1, BnPAP17-2, BnPAP17-3 and AtPAP17 as revealed on nucleotide scale (Table 1). BnPAP17 proteins also share 55-63%/73-80% of identities/positives to yellow lupine LlPAP (**CAE85073**), IbPAP, StPAP1, GmPAP and PvPAP, with significant similarities mainly at the C-terminal region.

Figure 2. Multi-alignment of amino acid sequences of AtPAP17 and the 3 BnPAP17 proteins. In the consensus line, the predicted conserved metallophos (pfam00149) domain between F_{48} and C_{256} is dash-underlined, the predicted signal peptide is solid-underlined, five motifs of conserved amino acid sequences (GDWG, GDNFY, GNHD, VVGH, and GHDH) are in gray background, those conserved metal-binding residues (D_{52}, D_{85}, Y_{88}, N_{123}, H_{217}, H_{252} and H_{254} in BnPAP17-1, and D_{48}, D_{81}, Y_{84}, N_{119}, H_{213}, H_{248} and H_{250} in BnPAP17-2 and BnPAP17-3) are boxed.

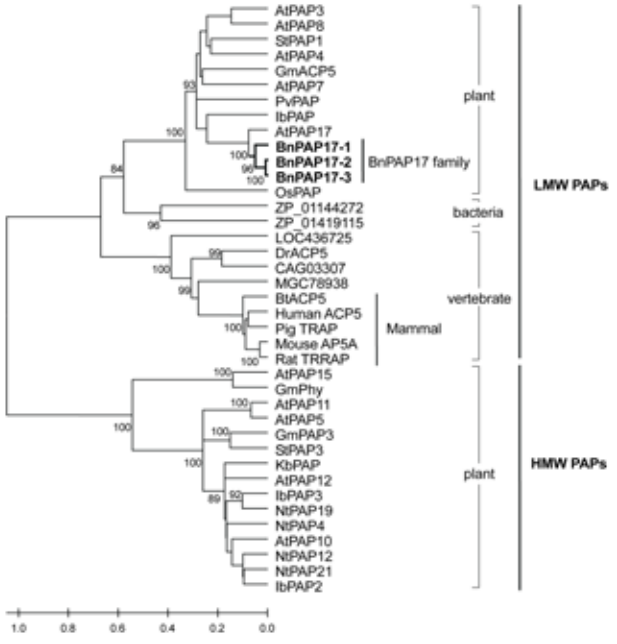

Figure 3 shows the phylogenetic relationships of BnPAP17 proteins with PAPs from plants and other kingdoms based on ClustalX alignment and Neighbor-Joining construction. Conforming to previous reports (Zimmermann et al., 2004), these PAPs were classified into 2 major groups (LMW PAPs and HMW PAPs), and the LMW PAPs could be further divided into 3 distinct subgroups (plant LMW PAPs, bacterial PAPs and vertebrate PAPs). The BnPAP17 family is grouped with AtPAP17 to form a highly related cruciferous cluster within the LMW PAP subgroup. Deduced plant PAPs such as AtPAP3, AtPAP4 and AtPAP8, GmPAP, PvPAP and StPAP1 are also grouped within the plant LMW PAP subgroup (Schenk et al., 2000a; Li et al., 2002; Zimmermann et al., 2004). NCBI Conserved Domain (CDD) search detected a metallophos (pfam00149) conserved domain located at the C-terminal region of BnPAP17 proteins. The domain resides between F_{47} and C_{255} of BnPAP17-1 with 89.5% alignments of the 184-residue CD-Length and F_{43}-C_{251} of BnPAP17-2 and

Figure 3. Phylogenetic relationship of deduced BnPAP17 proteins and related PAPs. Plant PAP sequences are: *A. thaliana* AtPAP3 (**NP_172923**), AtPAP4 (**NP_173894**), AtPAP5 (**NP_564619**), AtPAP7 (**NP_178297**), AtPAP8 (**NP_973397**), AtPAP10 (**NP_179235**), AtPAP11 (**NP_179405**), AtPAP12 (**NP_180287**), AtPAP15 (**NP_187369**) and AtPAP17 (**NP_566587**), *Solanum tuberosum* StPAP1 (**AAT37529**) and StPAP3 (**AAT37528**), *Glycine max* GmACP5 (**AAF60316**), GmPAP3 (**AAN85416**) and GmPhy (**AAK49438**), *Phaseolus vulgaris* PvPAP (**AAF60317**) and KbPAP (**P80366**), *Ipomoea batatas* IbPAP (**AAF60315**), IbPAP2 (**AAF19822**) and IbPAP3 (**CAA07280**), *Oryza sativa* OsPAP (**AAL34937**), *Nicotiana tabacum* NtPAP12 (**BAC55155**) and NtPAP21 (**BAC55157**). Vertebrate PAPs are: *Danio rerio* hypothetical protein LOC436725 (**NP_001002452**) and DrACP5 (**NP_999938**), *Tetraodon nigroviridis* (**CAG03307**), *Xenopus laevis* MGC78938 protein (**AAH72062**), *Bos taurus* BtACP5 (**B27035**), *Homo sapiens* Human ACP5 (**P13686**), *Sus scrofa* Pig TRAP (**P09889**), *Mus musculus* Mouse AP5A (**Q05117**), *Rattus norvegicus* Rat TRRAP (**P29288**). Bacterial PAPs are: *Acidiphilium cryptum JF-5* (**ZP_01144272**) and *Caulobacter* sp. K31 (**ZP_01419115**). The analysis is performed with ClustalX program and Mega program, and the tree is constructed by Neighbor-Joining method with *p*-distance. The number for each interior branch is the percent bootstrap value (1000 replicates), and only values greater than 80% are shown. The scale bar indicates the estimated number of amino acid substitutions per site.

BnPAP17-3 with 89.5% alignments for both (Figure 2). Within this domain, the 3 BnPAP17 proteins bear the same 5-block conserved motifs and 7 metal-binding residues (G**D**$_{52}$WG, G**D**$_{85}$NF**Y**$_{88}$, G**N**$_{123}$HD, VVG**H**$_{217}$ and G**H**$_{252}$D**H**$_{254}$, bold letters for metal-ligating residues) corresponding to those reported previously (Del Pozo et al., 1999). These features suggest that the 3 BnPAP17 proteins are typical plant LMW PAPs.

SignalP 3.0 analysis suggests that BnPAP17-1, BnPAP17-2 and BnPAP17-3 each possess a signal peptide, with the most likely cleavage sites at G_{30}-E_{31}, G_{26}-Q_{27} and G_{26}-E_{27}, respectively. TargetP 1.1, WoLFPSORT (http://wolfpsort.seq.cbrc.jp/) and PSORT also predict that these proteins are secreted. Based on predictions by TMpred, TMHMM and ConPred II (http://bioinfo.si.hirosaki-u.ac.jp/~ConPred2/), BnPAP17 proteins all have a significant N-terminal transmembrane helix occupying the main part of their signal peptides, e.g. from L_7/T_8 to V_{27}/T_{28}/N_{29} of BnPAP17-1, from T_5/L_7 to M_{23}/N_{25}/Q_{29} of BnPAP17-2, and from T_5/L_7 to M_{23}/N_{25}/Q_{29} of BnPAP17-3. Thus, it is likely that the 3 BnPAP17 proteins are extracellular proteins, like the reported AtPAP17 (Del Pozo et al., 1999).

Glycosylation is a typical feature of secreted plant enzymes including PAPs (Olczak et al., 2003). NetNGlyc 1.0 predicted that the 3 BnPAP17 proteins all have a potential N-glycosylation site NQSK. NetPhos 2.0 predicted 22-28 significant phosphorylation sites in each BnPAP17 member (13-16 for S, 5-7 for T, and 4-5 for Y), suggesting that phosphorylation may also be involved in functional regulation of them.

Analysis of secondary and tertiary structures of BnPAP17 proteins

Based on SOPMA prediction, BnPAP17-1, BnPAP17-2 and BnPAP17-3 contain 34.72%, 35.44% and 31.83% of random coils, 29.97%, 31.53% and 31.83% of alpha helices, 27.89%, 25.23% and 27.93% of extended strands, and 7.42%, 7.81% and 8.41% of beta turns, respectively (Figure 4). They all have 9 sites of obvious alpha helices and 15-16 sites of obvious extended strands along the whole molecule. It is noteworthy that there are 5 alpha helices in the metallophos domain, and 6 of 7 metal-binding sites are composed of random coil.

Crystal structures have been dissected for some plant HMW PAPs (such as KbPAP and IbPAP1) and some animal LMW PAPs, e.g. pig (PDB ID code 1UTE) and rat (PDB ID code 1QHW) (Schenk et al., 2005). Tertiary structures of BnPAP17 proteins were predicted by SWISS-MODEL based on their 28%-29% identities to 1UTE and 1QHW (Schwede et al., 2003). Displayed by Swiss-PdbViewer 3.7 (SP5), BnPAP17 proteins are similar to one another, especially that BnPAP17-2 and BnPAP17-3 show only a slight difference at β_4-α_5 (Figure 5). For BnPAP17 proteins, the main body is composed of 2 large sandwiched β-α-β-α-β folds (β_1-α_1-β_2-α_2-β_3 and β_6-α_5-β_7-α_6-β_8). Each sandwiched fold contains 3 parallel strands (β_1-β_2-β_3 and β_6-β_7-β_8), and the 2 sandwiched folds are connected by 2 small helices (α_3-α_4). Based on homologous alignment, the binuclear metal centers of BnPAP17 proteins might involve the D_{52}-Y_{88}-H_{254} coordination and the N_{123}-H_{217}-H_{252} coordination to bind the 2 ions, and the 2 metal ions in the active centers are bridged by the carboxylate group of D_{85}. The predicted tertiary structures proved these residues and signified 2 Fe ion binding centers (Figure 5).

Expression of the 3 *BnPAP17* genes in various organs tested

Expression of each *BnPAP17* gene family member could be detected in all tested organs by 31-cycle RT-PCR, with the highest in bud, followed by flower and 10D seed, while lowest in cotyledon (Figure 7). For organ specificity, though the 3 *BnPAP17* genes show similar trends, *BnPAP17-2* is more similar to *BnPAP17-3* than either to *BnPAP17-1*, consistent with their sequence similarity

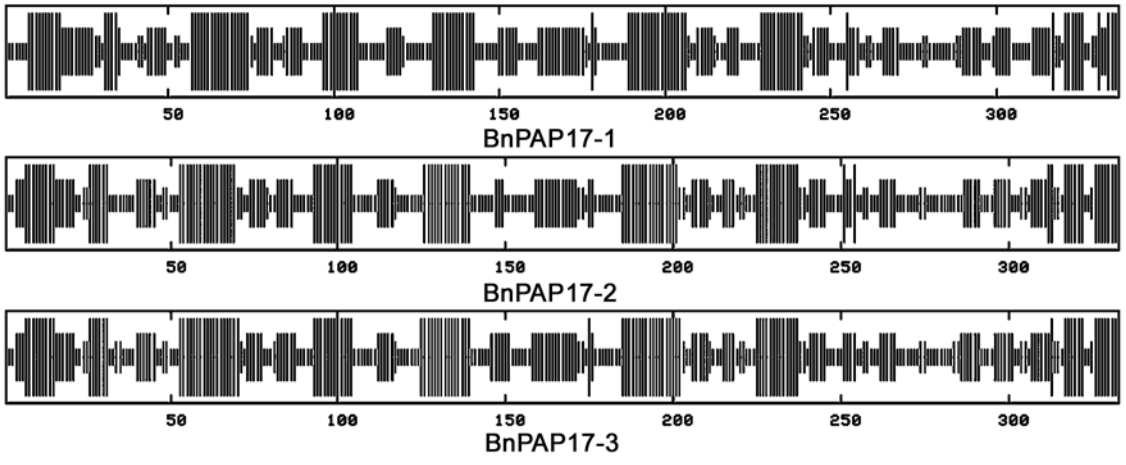

Figure 4. Predicted secondary structures of BnPAP17 proteins. Numbers 50, 100, etc., are counts of amino acids of each protein. α-helix, extended strand, β-turn and random coil are denoted as the longest, middle long, short and the shortest vertical bars respectively.

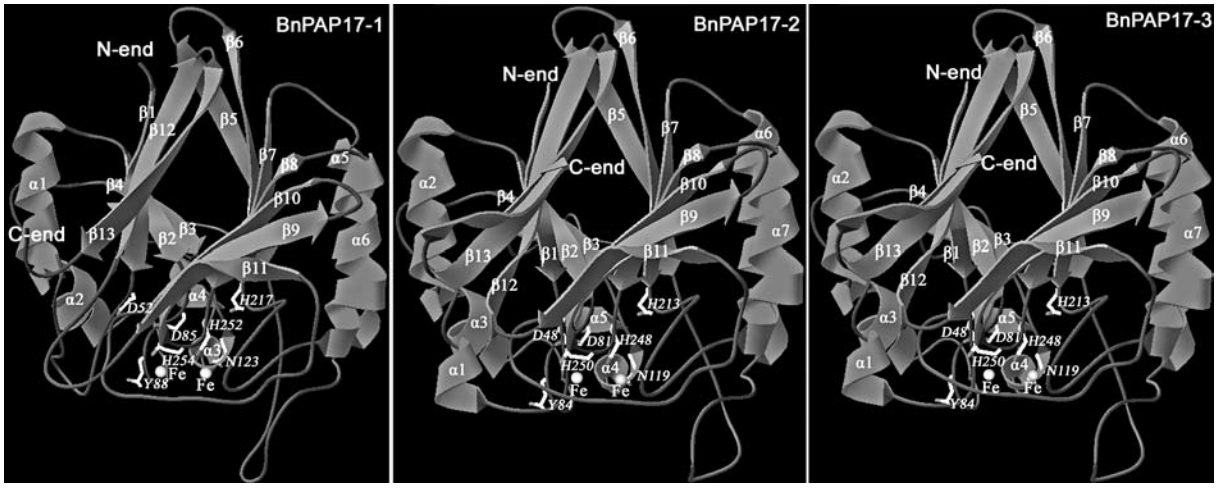

Figure 5. Tertiary structures of BnPAP17-1, BnPAP17-2 and BnPAP17-3. Pig LMW PAP (1UTE) was used as the model in SWISS-MODEL prediction, and Swiss-PdbViewer was adopted to show the results.

relationships. *BnPAP17-1* is more organ-specific, while *BnPAP17-2* and *BnPAP17-3* are more constitutive. The highest transcript level of *BnPAP17-1* could be detected in bud, followed by 10D seed, flower, silique pericarp and root, whereas its expression is weak in 20D seed and 30D seed and almost non-detectable in hypocotyl, cotyledon, stem and leaf. *BnPAP17-2* and *BnPAP17-3* also show the strongest expression in bud, followed by flower, stem, root, 10D seed, hypocotyl, silique pericarp, leaf, and cotyledon. While *BnPAP17-2* shows weak expression in 20D seed and 30D seed, *BnPAP17-3* is almost undetectable in these 2 stages of seed.

Pi-starvation induced expression of *BnPAP17* genes

The Pi-starvation induced expression patterns of *BnPAP17* family genes in seedling leaf (SL) and seedling root (SR) were determined in line W17 treated for 0 h, 12 h, 24 h, 2 d, 4 d and 8 d of Pi-starvation and 4 d of Pi resupply respectively. Only small amounts of *BnPAP17* transcripts could be observed in SL and SR under Pi-sufficient conditions (Figure 8). Under Pi-starvation conditions, similar induction trends could be observed between SL and SR. After 12 h of Pi-starvation, slight induction could be observed both in SL and SR. The expression levels continuously increased with time, and reached the maximal levels after 8 d of treatment, which was the most severe stress in this study. After 4 d of Pi resupply, *BnPAP17* expression dropped to near the basal levels. *BnPAP17-2* and *BnPAP17-3* showed similar trends to each other, but *BnPAP17-1* differed in that it returned to basal levels more slowly after Pi resupply. In SR, *BnPAP17-1* could be induced to an early peak level after 24 h of induction, while *BnPAP17-2* and *BnPAP17-3* needed 2 d.

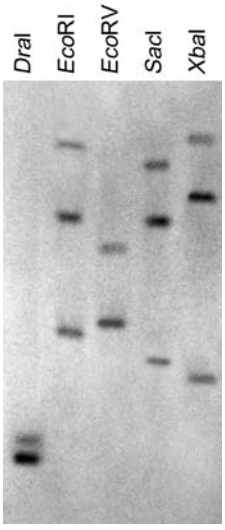

Figure 6. Southern hybridization detection of homologous *BnPAP17* members in *B. napus*.

DISCUSSION

Possible gene loss of the triplicated *PAP17* genes in *Brassica* ancestor

There were close evolutionary relationship and strong colinearity between the genomes of *Brassica* sepcies and *Arabidopsis* (Lagercrantz and Lydiate, 1996). The ancestor of *Brassiceae* triplicated its genome 13-17 million years ago (MYA), very soon after its divergence from the ancestor of genus *Arabidopsis* about 17-18 MYA (Yang et al., 2006). "Diploid" *Brassica* species such as *B. oleracea* and *B. rapa* are likely derived from a hexaploid ancestry (Lukens et al., 2004). Their genomes contain 3 representations of a basic genome, with each representation being extensively collinear with *A. thaliana* genome (Lysak et al., 2005). *Brassica napus* genome (1132 Mbp, 2n=38) is an amphidiploid of *B. rapa* AA-genome (529 Mbp, 2n=20) and *B. olerala* CC-genome (696 Mbp, 2n=18), and is more than 6 times of the *A. thaliana* genome (157 Mbp, 2n=10) (Johnston et al., 2005). It

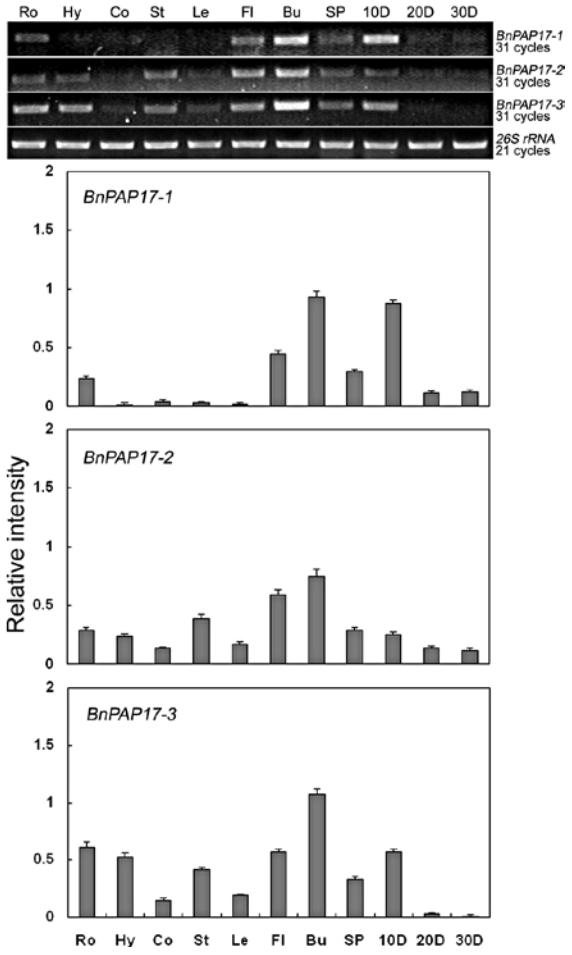

Figure 7. Tissue specificities of *BnPAP17* genes in various organs tested. Ro: root; Hy: hypocotyl; Co cotyledon; St: stem; Le: leaf; Fl: flower; Bu: bud; SP: silique pericarp; 10D: seed of 10 D; 20D: seed of 20 D; and 30D: seed of 30 D. Band intensities (columns) were normalized to *26S rRNA* band intensity and expressed as relative transcript level. Error bars indicate standard deviation (n=3).

is suggested that in *B. napus* there might exist about 6 orthologous genes corresponding to each gene from *A. thaliana* (Cavell et al., 1998).

In this study, 3 *BnPAP17* genes were isolated from *B. napus*, and Southern analysis also detected just 3 (*Eco*RI, *Sac*I and *Xba*I) or 2 (*Dra*I and *Eco*RV) hybridization bands. *BnPAP17-1* shares only ~77% genomic identities to the highly homologous *BnPAP17-2*/*BnPAP17-3* sisters. As the probe was a labeled *BnPAP17-1* full-length cDNA, the thickest band in each digestion may represent *BnPAP17-1* itself, while the weaker band(s) may represent *BnPAP17-2* or/and *BnPAP17-3*. The Southern hybridization result is in good agreement with the cloned 3 members, thus it could be postulated that *B. napus* probably contains only the 3 *BnPAP17* genes isolated here.

AtPAP17, *BnPAP17-1*, and *BnPAP17-2*/*BnPAP17-3* form a nearly triangle relationship among them in pairwise alignments, since *AtPAP17* is 77.2% identical to *BnPAP17-1* and 73.4%/73.5% identical to *BnPAP17-2*/*BnPAP17-3* while *BnPAP17-1* is 77.0%/77.2% identical to *BnPAP17-2*/*BnPAP17-3*. *BnPAP17-1* is a little more orthologous to *AtPAP17* than the other 2 members do. In the phylogenetic tree constructed using protein sequences, the 3 BnPAP17 proteins group together first and then with AtPAP17 soon. So it is obvious that a duplication event (most probably one event of the "triplication") right after the *Arabidopsis-Brassiceae* split resulted in the origination of *BnPAP17-2*/*BnPAP17-3* from *BnPAP17-1*. Loci in *B. napus* usually occur in homoeologous pairs, one originating from *B. rapa* AA genome and another from *B. oleracea* CC genome (Parkin et al., 2003). *BnPAP17-2* and *BnPAP17-3* show high similarities in sequence structures, tissue specificities and induced expression patterns, so they are probably from respective subgenome-donor species, i.e. they were orthologous to each other before the AA-CC fusion.

From above analysis, it can be assumed that gene loss might have occurred on the triplicated *PAP17* genes in *Brassica* ancestor, and current *B. rapa* and *B. oleracea* both might have only 1-2 *PAP17* genes. But this assumption needs to be identified by comparative cloning of *PAP17* genes from the 2 subgenome-donor species.

Several gene structure features deserve further study

Alternative transcriptional initiation and polyadenylation sites. *BnPAP17-1* has 4 alternative transcriptional initiation sites (A_1, A_{31}, T_{32} and A_{34}) and 4 alternative polyadenylation sites (C_{1457}, C_{1462}, T_{1463} and C_{1466}), and *BnPAP17-2* also has 2 alternative polyadenylation sites (T_{1579} and T_{1600}) (Figure 1). Length of UTRs may influence the mRNA stability and translation efficiency.

Conservative and variable regions in the 5′ UTRs. The ~70-bp region just prior to the start codon ATG is highly variable among *AtPAP17*, *BnPAP17-1* and *BnPAP17-2/BnPAP17-3* (Figure 1). In conservative motifs 2 and 5, *BnPAP17-1* is more similar to *AtPAP17* than to *BnPAP17-2/BnPAP17-3*, while in some other 5′ UTR short motifs *BnPAP17-1* is distinct from *AtPAP17* and *BnPAP17-2/BnPAP17-3*. These imply possible directional evolution of the start codon context for certain regulatory patterns in distinct *PAP17* genes. The 11-bp motif 1 (CTCCCTCCTTC) and the 13-bp motif 3 (CTCTCT(A/C)TTTCTC) is pyrimidine-rich and highly conservative, implying possible important *cis*-element of *PAP17* genes. However, the 21-bp purine-rich motif 4 (AGAGA(A/T)AGAGA(T/G)ATACAGATT) is just conserved among *BnPAP17* genes, suggesting its possible role in species-specific regulation. Like *B. napus F3′H-1* (Xu et al., 2007), the first 121, 69, and 69 bp of 5′ UTRs of *BnPAP17-1*, *BnPAP17-2* and *BnPAP17-3* respectively are also G-poor. These features offer structural models for investigating 5′ UTR *cis*-elements involved in transcription or translation of *PAP17*-type genes.

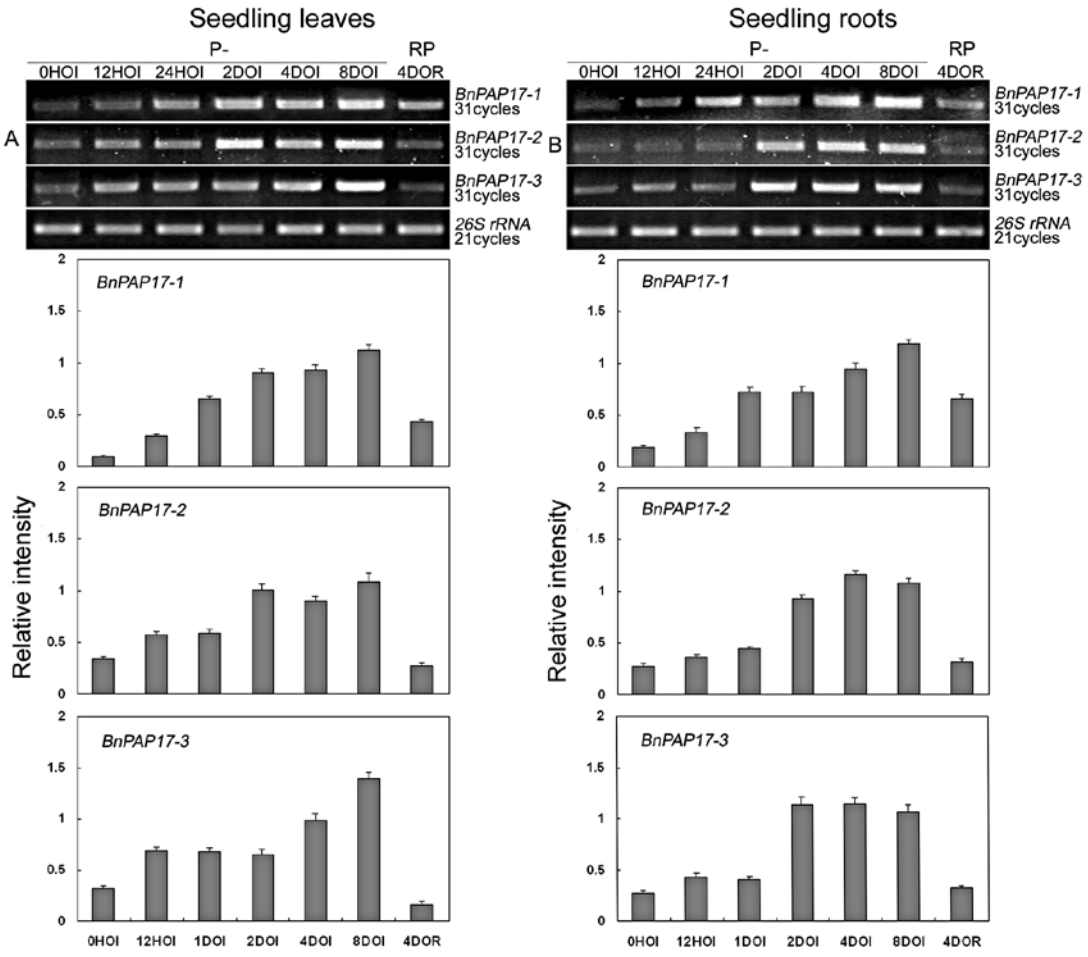

Figure 8. Pi-starvation induced expression patterns of *BnPAP17* gene family. SL (A) and SR (B) were sampled after 0 h, 12 h, 24 h, 2 d, 4 d and 8 d of Pi-starvation treatments (P-) and 4 d after Pi resupply (RP), respectively. HOI: h of induction; DOI: d of induction; DOR: d of Pi resupply. Band intensities (columns) were normalized to *26S rRNA* band intensity and expressed as relative transcript level. Error bars indicate standard deviation (n=3).

3′ UTR conserved motifs. Within the variable 3′ UTR, a cononical polyadenylation signal AATAAA and a 26-bp T-rich motif 6 (GTTT(C/T)TTTGTAATTTTTGTAACATAT) are also conserved among *PAP17* genes analysed (Figure 1). These kinds of motifs are suggested essential for accurate and efficient 3′-end formation (Ingelbrecht et al., 1989).

Conserved intron splicing border sequences. Most introns in nuclear mRNA precursors follow GT… AG splicing sites, but further structure features should be involved in (Breathnach and Chambon, 1981). The 2 introns are highly variable among *AtPAP17*, *BnPAP17-1* and *BnPAP17-2/BnPAP17-3*, but their border sequences are relatively conserved especially at the right borders. The "3′-intron|5′-exon" boundary sequences "intron I-TACAG|ATGGGAA-exon II" and "intron II-GATGCAG|T-exon III" might be important for proper intron splicing of *PAP17* genes.

Intron retention. Alternative splicing creates diversification of mRNA and protein products from a gene and defines a means of genetic regulation (Black, 2003). Intron retention is assumed to be an ancient form of alternative splicing in plants (Ast, 2004). In *Arabidopsis*, about 30% of alternatively spliced gene products were reported as intron retention (Ner-Gaon et al., 2004). In cloning of *B. napus* phenylpropanoid pathway genes, intron retention is often found on regulatory loci such as *TT2* (Wei et al., 2007). In this study, phenomenon of intron retention was detected in *BnPPA17-1* in GeneRacer handling. The encoded 76-aa premature polypeptide *BnPPA17-1PM* should be catalytically non-active as it lacks almost the whole metallophos domain (Figure 1). Since most of capped and polyadenylated *BnPPA17-1* mRNA molecules are normally spliced, and BnPPA17-1PM is unlikely to serve as a negative regulator, *BnPPA17-1PM* might be a result of leaky splicing.

Orthologous to AtPAP17, BnPAP17 proteins are typical plant LMW PAPs

Plant PAPs could be divided into LMW PAPs of ~35-kDa and HMW PAPs of ~55-kDa based on their MWs. Divergence between LMW PAPs and HMW PAPs

was a very early event, probably occurred before the plant-animal divergence (Del Pozo et al., 1999). In phylogenetic tree, BnPAP17 proteins are closer to bacterial and vertebrate PAPs rather than to plant HMW PAPs (Figure 4). So BnPAP17 proteins, which are 37.80-38.24 kDa, are typcal plant LMW PAPs. Resembling AtPAP17, all BnPAP17 proteins contain a metallophos domain, 5-block conserved motifs and 7 metal-binding residues typical for PAPs (Del Pozo et al., 1999). The OrthoMCL database (http://orthomcl.cbil.upenn.edu) searching revealed that BnPAP17 proteins have highest identities/positives (85%/92%) to ath14038 (AtPAP17). So, all *BnPAP17* genes are orthologous genes of *AtPAP17*, and could be assumed to be involved in Pi mobilization and in the metabolism of reactive oxygen species (Del Pozo et al., 1999).

As shown in Figure 5, BnPAP17 proteins are mainly composed of 2 large sandwiched β-α-β-α-β folds, which were connected by 2-3 continuous α helices, implying that BnPAP17 proteins have typical tertiary structure features of PAPs. The binuclear metal centers of pig and rat PAPs are Fe(III)-Fe(II) type, differring from Fe(III)-Zn(II) or Fe(III)-Mn(II) center from plants (Olczak et al., 2003). To date there is no report on crystal structure of plant LMW PAPs, and there is also no evidence about the actual metal ions bound in plant LMW PAPs. But the basic tertiary structure together with a Fe-Fe binding center of BnPAP17 proteins was still predicted out based on mammalian PAPs, suggesting that the core of three-dimensional structures of plant LMW PAPs basically resembles mammal PAPs.

Implied functional importance and diverged expression of *PAP17* genes

In *Arabidopsis*, although 28 *PAP* genes differed in their expression patterns in vegetative organs, but all transcribed in flower, strongly implying that *PAP* genes may play crucial roles in flower and seed development (Zhu et al., 2005). *AtPAP17* has been reported with the highest expression in senescent leaf, followed by flower, while weak expression in silique, root 1and stem (Del Pozo et al., 1999). However, systemic RT-PCR detection of *AtPAP*s indicated that *AtPAP17* has the highest expression in silique, while relatively low expression in root, stem, leaf and flower (Zhu et al., 2005). In this study, 11 different organs were adopted to detailedly characterize *BnPAP17* member-specific expression patterns. Favoring the results of Zhu et al. (2005), our results demonstrated that *BnPAP17* genes are also dominantly expressed in reproductive organs. But *BnPAP17* genes are most intensively transcribed in flower bud, though also intensive in mature flower and young seed (Figure 7). Combinatorially, our results support a very important role of *BnPAP17* genes in the development of reproductive organs of *B. napus* via their intensive expression through the whole reproductive developmental stages, i.e. from flower buds to mature flowers, then to developing seeds.

Our results also provide strong evidence suggesting the involvement of *BnPAP17* genes in Pi activation, absorption and inter-organ transferring especially to the developing reproductive organs in *B. napus*. First, relatively high expression of *BnPAP17* gene family was detected in vascular tissues such as root, hypocotyl and stem, then a path from root to vascular tissue then to reproductive organs can be imagined along which *BnPAP17* genes show intensive expression. Second, expression of *BnPAP17* genes are strongly induced by Pi-starvation. The degree of induction increased along with the severity of the stress, and rapidly returned to near basal levels after Pi resupply. Similar Pi resupply expression trend of *AtPAP17* was reported by Del Pozo et al. (1999). Muller et al. (2004) also demonstrated that *AtPAP17* showed a clear reduction in transcript level after 1 h of Pi resupply, especially in roots notable decrease only required 30 min, preceding the change in shoots. The activity of *AtPAP17* has been used as a marker for Pi deficiency researches in *Arabidopsis* (Muller et al., 2004; Todd et al., 2004). Our results basically conform to those of *AtPAP17*. Third, the response of *BnPAP17* genes to Pi-starvation was faster in SL than in SR, which is in agreement with *AtPAP12* (Haran et al., 2000). The most possible implication of the phenomenon is that plants usually strive to utilize endogenous P storage pools in the shoots by mediating APase activity before to hydrolyze organic P complex in soils via activation of APase in roots (Haran et al., 2000).

In this study, *BnPAP17* members show distinct differences in tissue specificities. *BnPAP17-2* and *BnPAP17-3* show more similar organ specificity than either to *BnPAP17-1*. *BnPAP17-1* is more organ-specific, and *BnPAP17-2* and *BnPAP17-3* are more widely expressed. Besides important roles in developing reproductive organs, intensive expression of *BnPAP17-2* and *BnPAP17-3* in vascular tissues also indicates their roles in Pi absorption, activation and transferring. However, the expression of *BnPAP17-1* is more limited to reproductive organs, and root is the only vegetative organ with intensive expression, implying its possible major roles in aspects of Pi metabolism except long-distance Pi transferring. These, together with the certain difference of organ specificity between *AtPAP17* and *BnPAP17* family, suggest both orthologous and paralogous divergence of expression patterns of *PAP17* genes, maybe for functional division, complementation, and diversification.

Acknowledgements. This work was supported financially by the National High Technology Research and Development Program of China (863 Program) (Grant No. 2006AA10A113 and 2006AA100106).

LITERATURE CITED

Ast, G. 2004. How did alternative splicing evolve? Nat. Rev. Genet. **5:** 773-782.

Black, D.L. 2003. Mechanisms of alternative pre-messenger RNA splicing. Annu. Rev. Biochem. **72:** 291-336.

Breathnach, R. and P. Chambon. 1981. Organization and expression of eukaryotic split genes coding for proteins. Ann. Rev. Biochem. **50:** 349-383.

Cavell, A.C., D.J. Lydiate, I.A.P. Parkin, C. Dean, and M. Trick. 1998. Collinearity between a 30-centimorgan segment of *Arabidopsis thaliana* chromosome 4 and duplicated regions within the *Brassica napus* genome. Genome **41:** 62-69.

Del Pozo, J.C., I. Allona, V. Rubio, A. Leyva, A. de la Pena, C. Aragoncillo, and J. Paz-Ares. 1999. A type 5 acid phosphatase gene from *Arabidopsis thaliana* is induced by phosphate starvation and by some other types of phosphate mobilising/oxidative stress conditions. Plant J. **19:** 579-589.

Guo, Y.C., W.X. Lin, Q.M. Shi, Y.Y. Liang, F.G. Chen, H.Q. He, and K.J. Liang. 2002. Screening methodology for rice (*Oryza sativa*) genotypes with high phosphorus use efficiency at their seedling stage. Chin. J. Appl. Ecol. **13:** 1587-1591. (in Chinese)

Haran, S., S. Logendra, M. Seskar, M. Bratanova, and I. Raskin. 2000. Characterization of *Arabidopsis* acid phosphatase promoter and regulation of acid phosphatase expression. Plant Physiol. **124:** 615-626.

Hoagland, D.R. and D.L. Arnon. 1950. The water culture method for growing plants without soil. Calif. Agric. Exp. Sta. Circ. **347:** 32.

Ingelbrecht, I.L.W., L.M.F. Herman, R.A. Dekeyser, M.C. Van Montagu, and A.G. Depicker. 1989. Different 3′ end regions strongly influence the level of gene expression in plant cells. Plant Cell **1:** 671-680.

Jaakola, L., A.M. Pirttil, M. Halonen, and A. Hohtola. 2001. Isolation of high quality RNA from bilberry (*Vaccinium myrtillus* L.) fruit. Mol. Biotechnol. **19:** 201-203.

Johnston, J.S., A.E. Pepper, A.E. Hall, Z.J. Chen, G. Hodnett, J. Drabek, R. Lopez, and H.J. Price. 2005. Evolution of genome size in Brassicaceae. Ann. Bot. (Lond). **95:** 229-235.

Kaida, R., K. Sage-Ono, H. Kamada, H. Okuyama, K. Syono, and T.S. Kaneko. 2003. Isolation and characterization of four cell wall purple acid phosphatase genes from tobacco cells. Biochim. Biophys. Acta **1625:**134-140.

Klabunde, T., N. Strater, B. Krebs, and H. Witzel. 1995. Structural relationship between the mammalian Fe(III)-Fe(II) and the Fe(III)-Zn(II) plant purple acid phosphatases. FEBS Lett. **367:** 56-60.

Kumar, S., K. Tamura, and M. Nei. 2004. MEGA3: integrated software for molecular evolutionary genetics analysis and sequence alignment. Brief. Bioinform. **5:** 150-163.

Lagercrantz, U. and D.J. Lydiate. 1996. Comparative genome mapping in *Brassica*. Genetics **144:** 1903-1910.

Li, D., H. Zhu, K. Liu, X. Liu, G. Leggewie, M. Udvardi, and D. Wang. 2002. Purple acid phosphatases of *Arabidopsis thaliana*. Comparative analysis and differential regulation by phosphate deprivation. J. Biol. Chem. **277:** 27772-27781.

Liao, H., F.L. Wong, T.H. Phang, M.Y. Cheung, W.Y. Li, G. Shao, X. Yan, and H.M. Lam, 2003. *GmPAP3*, a novel purple acid phosphatase-like gene in soybean induced by NaCl stress but not phosphorus deficiency. Gene **318:** 103-111.

Lukens, L.N., P.A. Quijada, J. Udall, J.C. Pires, M.E. Schranz, and T.C. Osborn. 2004. Genome redundancy and plasticity within ancient and recent *Brassica* crop species. Biol. J. Linn. Soc. Lond. **82:** 665-674.

Lysak, M.A., M.A. Koch, A. Pecinka, and I. Schubert. 2005. Chromosome triplication found across the tribe Brassiceae. Genome Res. **15:** 516-525.

Muller, R., L. Nilsson, C. Krintel, and T.H. Nielsen. 2004. Gene expression during recovery from phosphate starvation in roots and shoots of *Arabidopsis thaliana*. Physiol. Plant. **122:** 233-243.

Ner-Gaon, H., R. Halachmi, S. Savaldi-Goldstein, E. Rubin, R. Ophir, and R. Fluhr. 2004. Intron retention is a major phenomenon in alternative splicing in *Arabidopsis*. Plant J. **39:** 877-885.

Oddie, G.W., G. Schenk, N.Z. Angel, N. Walsh, L.W. Guddat, J. de Jersey, A.I. Cassady, S.E. Hamilton, and D.A. Hume. 2000. Structure, function, and regulation of tartrate-resistant acid phosphatase. Bone **27:** 575-84.

Olczak, M., B. Morawiecka, and W. Watorek. 2003. Plant purple acid phosphatases- genes, structures and biological function. Acta Biochim. Pol. **50:** 1245-1256.

Parkin, I.A.P., A.G. Sharpe, and D.J. Lydiate. 2003. Patterns of genome duplication within the *Brassica napus* genome. Genome **46:** 291-303.

Saghai-Maroof, M.A., K.M. Soliman, R.A. Jorgensen, and R.W. Allard. 1984. Ribosomal DNA spacer-length polymorphisms in barley: mendelian inheritance, chromosomal location, and population dynamics. Proc. Natl. Acad. Sci. USA **81:** 8014-8018.

Schenk, G., L.R. Gahan, L.E. Carrington, N. Mitic, M. Valizadeh, S.E. Hamilton, J. de Jersey, and L.W. Guddat. 2005. Phosphate forms an unusual tripodal complex with the Fe-Mn center of sweet potato purple acid phosphatase. Proc. Natl. Acad. Sci. USA **102:** 273-278.

Schenk, G., L.W. Guddat, Y. Ge, L.E. Carrington, D.A. Hume, S. Hamilton, and J. de Jersey. 2000a. Identification of mammalian-like purple acid phosphatases in a wide range of plants. Gene **250:** 117-125.

Schenk, G., M.L. Korsinczky, D.A. Hume, S. Hamilton, and J. de Jersey, 2000b. Purple acid phosphatases from bacteria: similarities to mammalian and plant enzymes. Gene **255:** 419-24.

Schwede, T., J. Kopp, N. Guex, and M.C. Peitsch. 2003. SWISS-MODEL: an automated protein homology-modeling server. Nucleic Acids Res. **31:** 3381-3385.

Singh, K., J. Raizada, P. Bhardwaj, S. Ghawana, A. Rani, H. Singh, K. Kaul, and S. Kumar. 2004. 26S rRNA-based internal control gene primer pair for reverse transcription-polymerase chain reaction-based quantitative expression studies in diverse plant species. Anal. Biochem. **335:** 330-333.

Strater, N., T. Klabunde, P. Tucker, H. Witzel, B. Krebs. 1995. Crystal structure of a purple acid phosphatase containing a dinuclear Fe(III)-Zn(II) active site. Science **268:** 1489-1492.

Thompson, J.D., T.J. Gibson, F. Plewniak, F. Jeanmougin, and D.G. Higgins. 1997. The CLUSTAL_X windows interface: flexible strategies for multiple sequence alignment aided by quality analysis tools. Nucleic Acids Res. **25:** 4876-4882.

Todd, C.D., P. Zeng, A.M.R. Huete, M.E. Hoyos, and J.C. Polacco. 2004. Transcripts of MYB-like genes respond to phosphorous and nitrogen deprivation in *Arabidopsis*. Planta **219:** 1003-1009.

Vincent, J.B., M.W. Crowder, and B.A. Averill. 1992. Hydrolysis of phosphate monoesters: a biological problem with multiple chemical solutions. Trends Biochem. Sci. **17:** 105-110.

Wasaki, J., M. Omura, M. Ando, H. Dateki, T. Shinano, M. Osaki, H. Ito, H. Matsui, and T. Tadano. 2000. Molecular cloning and root specific expression of secretory acid phosphatase from phosphate deficient lupin (*Lupinus albus* L.) Soil Sci. Plant Nutr. **46:** 427-437.

Wasaki, J., M. Omura, M. Osaki, H. Ito, H. Matsui, T. Shinano, and T. Tadano. 1999. Structure of a cDNA for an acid phosphatase from phosphate-deficient lupin (*Lupinus albus* L.) roots. Soil Sci. Plant Nutr. **45:** 433-439.

Wei, Y.L., J.N. Li, J. Lu, Z.L. Tang, D.C. Pu, and Y.R. Chai. 2007. Molecular cloning of *Brassica napus TRANSPARENT TESTA 2* gene family encoding potential MYB regulatory proteins of proanthocyanidin biosynthesis. Mol. Biol. Rep. **34:** 105-120.

Xiao, K., M. Harrison, and Z.Y. Wang. 2006. Cloning and characterization of a novel purple acid phosphatase gene (*MtPAP1*) from *Medicago truncatula* Barrel Medic. J. Int. Plant Biol. **48:** 204-211.

Xu, B.B., J.N. Li, X.K. Zhang, R. Wang, L.L. Xie, and Y.R. Chai. 2007. Cloning and molecular characterization of a functional flavonoid 3´-hydroxylase gene from *Brassica napus*. J. Plant Physiol. **164:** 350-363.

Yang, G.Z., Y. Zhang, R.Q. Wang, Y.L. Yao, and Z. Song. 2007. Study on high-yielding cultivation model for *Brassica napus* L. 12th International Rapeseed Congress, Wuhan, China, Science Press USA Inc., pp. 18-21.

Yang, T.J., J.S. Kim, S.J. Kwon, K.B. Lim, B.S. Choi, J.A. Kim, M. Jin, J.Y. Park, M.H. Lim, and H.I. Kim. 2006. Sequence-level analysis of the diploidization process in the triplicated *FLOWERING LOCUS C* region of *Brassica rapa*. Plant Cell **18:** 1339-1347.

Zhu, H., W. Qian, X. Lu, D. Li, X. Liu, K. Liu, and D. Wang. 2005. Expression patterns of purple acid phosphatase genes in *Arabidopsis* organs and functional analysis of *AtPAP23* predominantly transcribed in flower. Plant Mol. Biol. **59:** 581-594.

Zimmermann, P., B. Regierer, J. Kossmann, E. Frossard, N. Amrhein, and M. Bucher, 2004. Differential expression of three purple acid phosphatases from potato. Plant Biol. (Stuttg). **6:** 519-528.

甘藍型油菜潛在的紫色酸性磷酸酶 *17*（*BnPAP17*）基因家族的克隆、分析和磷饑餓誘導表達

盧　坤[1]　李加納[1]　鐘巍然[1]　張　凱[1]　付福友[2]　柴友榮[1]

[1]西南大學農學與生物科技學院，重慶市油菜工程技術研究中心，重慶市作物品質改良重點實驗室，農業部生物技術與作物品質改良重點實驗室

[2]中國科學院遺傳與發育生物學研究所，植物基因組學國家重點實驗室

本研究克隆了甘藍型油菜紫色酸性磷酸酶 *PAP17*（*BnPAP17*）基因家族的 3 個成員。*BnPAP17-1*、*BnPAP17-2* 和 *BnPAP17-3* 的全長 cDNA 分別為 1277、1356 和 1349 bp，基因組序列分別為 1466、1594 和 1598 bp。推定的 BnPAP17-1、BnPAP17-2 和 BnPAP17-3 蛋白分別包含 337、333 和 333 個氨基酸殘基，它們均為分泌性低分子量（LMW）PAP，包含金屬磷（metallophos）結構域、5 個保守性基序和 7 個金屬離子結合殘基。*BnPAP17-2* 與 *BnPAP17-3* 高度相似，而它們與 *BnPAP17-1* 差異較大。Southern 雜交進一步證實這3個成員構成了整個 *BnPAP17* 家族。RT-PCR 分析表明 *BnPAP17* 家族成員主要在生殖器官中表達，尤以蕾中表達量最高。在營養器官中，*BnPAP17-2* 和 *BnPAP17-3* 在根、下胚軸和莖中有一定程度的表達，而 *BnPAP17-1* 只在根中表達。在苗期，它們均受磷饑餓強烈誘導，而恢復供磷後表達量回復到誘導前水準，表明這些成員在植株的生殖發育和對磷缺乏的適應性中發揮重要作用。

關鍵詞：甘藍型油菜；基因家族；紫色酸性磷酸酶；磷饑餓。